ISSN 1809-5860

BEM ANALYSIS OF POROUS MEDIA SUBJECTED TO DAMAGE: AN APPLICATION TO GEOMECHANICS

Eduardo Toledo de Lima Junior[1], Wilson Sergio Venturini[2], Ahmed Benallal[3]

Abstract

This work is devoted to the numerical analysis of saturated porous media, taking into account the damage phenomena on the solid skeleton. The porous media is taken into poro-elastic framework, in full-saturated condition, based on the Biot's Theory. A scalar damage model is assumed for this analysis. An implicit boundary element method (BEM) formulation, based on time-independent fundamental solutions, is developed and implemented to couple the fluid flow and two-dimensional elastostatic problems. The integration over boundary elements is evaluated by using a numerical Gauss procedure. A semi-analytical scheme for the case of triangular domain cells is followed to carry out the relevant domain integrals. The non-linear problem is solved by a Newton-Raphson procedure. Numerical examples are presented, in order to validate the implemented formulation and to illustrate its efficiency.

Keywords: Porous Media. Isotropic Damage. Boundary Element Method.

1 INTRODUCTION

The study of porous materials is extremely relevant in several areas of knowledge, such as soil and rock mechanics, contaminant diffusion, biomechanics and petroleum engineering. The mechanics of porous media deals with materials where the mechanical behavior is significantly influenced by the presence of fluid phases. The response of the material is highly dependent on the fluids that flow through the pores. BIOT (1941) was the first to propose a coupled theory for three-dimensional consolidation, based on the Terzaghi's studies on soil settlement (TERZAGHI, 1923). This thermodynamically consistent theory is described in the book by COUSSY (2004), who improved significantly the knowledge on poromechanics. CLEARY (1977) presented the fundamental solutions to porous solids, representing the first contributions on integral equations dedicated to this kind of problems. Among others pioneers BEM works applied to porous media, the ones from CHENG and his collaborators (1984,1987,1998) are well-known, using the direct BEM formulation.

In the field of material mechanics, we note the modelling of nonlinear physical processes, as damage and fracture. Processes of energy dissipation and consequent softening have been extensively studied, so that one can count on a wide range of models already developed. Continuum Damage Mechanics (CDM) deals with the load carrying capacity of solids whose material is damaged due to the presence of micro-cracks and micro-voids. CDM was originally conceived by KACHANOV (1958), to analyze uniaxial creeping of metals subjected to high-order temperatures. Several authors studied and developed models related to CDM. LEMAITRE and colleagues (1985,1992) contributed significantly to the field. In this work, we use the model of MARIGO (1981), who presented a scalar isotropic model for brittle and quasi-brittle materials. The first applications of BEM to damage mechanics reported in the literature are HERDING & KUHN (1996) and GARCIA et al (1999). Recently, we can cite the works of SLADEK et al. (2003), BOTTA et al. (2005) and BENALLAL et al. (2006). These works include non-local formulations to treat strain localization phenomena and associated numerical instabilities. Some aspects on the numerical analysis of porous media experiencing damage are found in CHENG & DUSSEAULT (1993) and SELVADURAI (2003).

[1] Professor in the Scientific Computing and Visualization Laboratory - UFAL, limajunior@lccv.ufal.br
[2] Professor in the Department of Structural Engineering - EESC-USP, *in memoriam*
[3] Research Director in the Mechanics and Technology Laboratory, ENS de Cachan, benallal@lmt.ens-cachan.fr

Due to the increasing complexity of models developed for engineering problems, robust numerical models capable to provide accurate results with the least possible computational effort are looked for. In this scenario, BEM appears as an interesting choice for obtaining numerical solutions in various engineering applications.

In this paper, a non-linear set of transient BEM equations is developed, based on Betti's reciprocity theorem, to deals with isotropic-damaged porous media. The description of porous solid is done in a Lagrangean approach. Marigo's damage model is applied with a local evaluation of the thermodynamic force associated to damage.

Regarding the BEM numerical procedure, the integration over boundary elements is evaluated by using a numerical Gauss procedure. A semi-analytical scheme for the case of triangular domain cells is followed to carry out the relevant domain integrals. A Newton-Raphson procedure is applied to solve the non-linear system, with a consistent tangent operator. This is done in the light of the procedure introduced by SIMO & TAYLOR (1985) for finite elements.

2 GOVERNING EQUATIONS

The following free energy potential is considered,

$$\rho\psi(\varepsilon_{jk}, \mathrm{D}, \phi-\phi_0) = \frac{1}{2}(1-\mathrm{D})\varepsilon_{jk}\mathrm{E}^{\mathrm{d}}_{jklm}\varepsilon_{lm} + \frac{1}{2}b^2 M\left[\mathrm{Tr}\left(\varepsilon_{jk}\right)\right]^2 + \frac{1}{2}M\left(\phi-\phi_0\right)^2 - bM\left(\phi-\phi_0\right)\mathrm{Tr}\left(\varepsilon_{jk}\right) \tag{1}$$

where the constants M and b represent the Biot modulus and Biot coefficient of effective stress, respectively. In the case of saturated media, filled by an incompressible fluid, the Biot coefficient assumes unit value. In full-saturated conditions, the lagrangian porosity ϕ measures the variation of fluid content per unit volume of porous material. The bulk density is described by ρ. $\mathrm{E}^{\mathrm{d}}_{jklm}$ represents the isotropic drained elastic tensor. ε_{jk} denotes the strains in the solid skeleton. Assuming isotropic case, the damage is represented by the scalar-valued internal variable D, which defines the internal state of the material, taking values between zero (sound material) and one (complete degradation). The initial porosity field is indicated by ϕ_0.

The derivatives of free energy potential with respect to the internal variables lead to the associate variables, that are the total stress σ_{jk}, the pore-pressure p and the thermodynamical force Y conjugated to D.

$$\sigma_{jk} = \rho\frac{\partial\psi}{\partial\varepsilon_{jk}} = (1-\mathrm{D})\mathrm{E}^{\mathrm{d}}_{jklm}\varepsilon_{lm} + bM\left[b\mathrm{Tr}\left(\varepsilon_{jk}\right) - \left(\phi-\phi_0\right)\right]\delta_{jk} \tag{2}$$

$$\left(\mathrm{p}-\mathrm{p}_0\right) = \rho\frac{\partial\psi}{\partial\left(\phi-\phi_0\right)} = M\left[\left(\phi-\phi_0\right) - b\mathrm{Tr}\left(\varepsilon_{jk}\right)\right] \tag{3}$$

$$Y = -\rho\frac{\partial\psi}{\partial\mathrm{D}} = \frac{1}{2}\varepsilon_{jk}\mathrm{E}^{\mathrm{d}}_{jklm}\varepsilon_{lm} \tag{4}$$

Using equations (2) and (3) the total stress tensor is written as

$$\sigma_{jk} = \mathrm{E}_{jklm}\varepsilon_{lm} - \mathrm{D}\mathrm{E}_{jklm}\varepsilon_{lm} - b\left(\mathrm{p}-\mathrm{p}_0\right)\delta_{jk} \tag{5}$$

from which it is seen that it includes three different contributions, being the first one the effective stress σ_{jk}^{ef}, acting on the grains of the solid matrix, and the second one the stress due to damage σ_{jk}^{d}.

In addition to the state laws given above, it is necessary to define a damage criterion. In Marigo's model it takes the form:

$$F(Y,\mathrm{D}) = Y - \kappa(\mathrm{D}) \tag{6}$$

The term $\kappa(\mathrm{D})$ represents the maximum value of Y reached during the loading history, and is adopted here in its simple linear form $\kappa(\mathrm{D}) = Y_0 + A\mathrm{D}$, where parameters Y_0 and A are material dependent. The damage evolution becomes from the consistency condition $\dot{F}(Y,\mathrm{D}) = 0$, resulting in:

$$\dot{\mathrm{D}} = \dot{Y}/A \tag{7}$$

The fluid flow through the porous space can be described by Darcy's law. Assuming a laminar flow, this law considers a linear relationship between the flow rate and the pressure gradient:

$$\nu_{\mathrm{k}} = \mathrm{k}\left[-\mathrm{p}_{,\mathrm{k}} + f_{\mathrm{k}}\right] \tag{8}$$

In this simple version, it is assumed isotropic, with $\mathrm{k} = \dfrac{k}{\mu}$ the scalar permeability coefficient, defined as a function of the intrinsic permeability k and the fluid viscosity μ. The fluid body force is represented by f_{k}.

The fluid mass balance equation, assuming no external fluid sources, is written as:

$$\frac{\mathrm{d}\left(\rho_{\mathrm{f}}\phi\right)}{\mathrm{dt}} + \left(\rho_{\mathrm{f}}\nu_{\mathrm{k}}\right)_{,\mathrm{k}} = 0 \tag{9}$$

The following equilibrium and compatibility relations, added to appropriate boundary conditions complete the set of equations that describes the poro-elasto-damage problem, in quasi-static conditions:

$$\sigma_{\mathrm{jk,k}} + \mathrm{b}_{\mathrm{j}} = 0 \tag{10}$$

$$\varepsilon_{\mathrm{jk}} = \frac{1}{2}\left(\mathrm{u}_{\mathrm{k,j}} + \mathrm{u}_{\mathrm{j,k}}\right) \tag{11}$$

3 INTEGRAL EQUATIONS

In order to couple the behaviour of the solid and fluid phases, two sets of integral equations are derived. The first one is related to the elastostatics problem, for which a pore-pressure field is distributed over the domain, while the other equation refers to the pore-pressure itself.

In order to obtain the integral equations one can use Betti's reciprocity theorem, which can only be applied to elastic fields. Thus, in the case of elasticity, assuming the effective stress definition:

$$\int_{\Omega} \sigma_{\mathrm{jk}}^{\mathrm{ef}}(\mathrm{q})\varepsilon_{\mathrm{ijk}}^{*}(\mathrm{s},\mathrm{q})\mathrm{d}\Omega = \int_{\Omega} \varepsilon_{\mathrm{jk}}(\mathrm{q})\sigma_{\mathrm{ijk}}^{*}(\mathrm{s},\mathrm{q})\mathrm{d}\Omega \tag{12}$$

$$\int_{\Omega}\left(\sigma_{jk}(q)+\sigma_{jk}^{d}(q)+b\delta_{jk}p(q)\right)\varepsilon_{ijk}^{*}(s,q)d\Omega=\int_{\Omega}\varepsilon_{jk}(q)\sigma_{ijk}^{*}(s,q)d\Omega \tag{13}$$

where s and q represent the source and field points, and X^{*} is the fundamental solution for the variable X, from now on. The direction i refers to the application of the unit load on the source point into the fundamental domain. In elastostatics, one applies the well-known Kelvin fundamental solutions. By applying the divergence theorem to equation (13), and considering the transient nature of the problem, one obtains the following integral equation for displacements on the boundary points S:

$$\begin{aligned}C_{ik}\dot{u}_{k}(S)&=\int_{\Gamma}\dot{t}_{k}(Q)u_{ik}^{*}(S,Q)d\Gamma-\int_{\Gamma}T_{ik}^{*}(S,Q)\dot{u}_{k}(Q)d\Gamma\\&+\int_{\Omega}b\delta_{jk}\dot{p}(q)\varepsilon_{ijk}^{*}(S,q)d\Omega+\int_{\Omega}\dot{\sigma}_{jk}^{d}(q)\varepsilon_{ijk}^{*}(S,q)d\Omega\end{aligned} \tag{14}$$

The stresses at internal points are obtained by differentiating equation (14), now written for internal points, and applying Hooke's law, which leads to

$$\begin{aligned}\dot{\sigma}_{ij}(s)&=-\int_{\Gamma}S_{ijk}(s,Q)\dot{u}_{k}(Q)d\Gamma+\int_{\Gamma}D_{ijk}(s,Q)\dot{t}_{k}(Q)d\Gamma+\int_{\Omega}R_{ijkl}(s,q)\dot{\sigma}_{kl}^{d}(q)d\Omega\\&+TL_{ij}\left[\dot{\sigma}_{kl}^{d}(s)\right]+\int_{\Omega}b\delta_{kl}R_{ijkl}(s,q)\dot{p}(q)d\Omega+TL_{ij}\left[b\delta_{kl}\dot{p}(s)\right]\end{aligned} \tag{15}$$

where S_{ijk}, D_{ijk} and R_{ijkl} are the derivatives of the fundamental solutions, and TL_{ij} are the free-terms coming from differentiation.

The integral equation for the pore-pressure can be obtained in a similar way, defining the proportional flow vector $v_{k}^{pr}=v_{k}-kf_{k}=-kp_{,k}$ in order to apply Betti's Theorem

$$\int_{\Omega}\left[v_{k}-kf_{k}\right]p_{,k}^{*}(s,q)d\Omega=\int_{\Omega}v_{k}^{*}(s,q)p_{,k}(q)d\Omega \tag{16}$$

from what the divergence theorem leads to write:

$$\begin{aligned}p(s)&=-\int_{\Gamma}v_{\eta}^{*}(s,Q)p(Q)d\Gamma+\int_{\Gamma}p^{*}(s,Q)v_{\eta}(Q)d\Gamma\\&-\int_{\Omega}p^{*}(s,q)v_{k,k}(q)d\Omega-\int_{\Omega}p_{,k}^{*}(s,q)kf_{k}(q)d\Omega\end{aligned} \tag{17}$$

η indicates the outward normal direction to the boundary. Assuming $v_{k,k}=-\dot{\phi}$ (see (9)) and, neglecting the body force f_{k}, we get:

$$p(s)=-\int_{\Gamma}v_{\eta}^{*}(s,Q)p(Q)d\Gamma+\int_{\Gamma}p^{*}(s,Q)v_{\eta}(Q)d\Gamma+\int_{\Omega}p^{*}(s,q)\dot{\phi}(q)d\Omega \tag{18}$$

For convenience, it is possible to take the derivative $\dot{\phi}(q)$ from (3), so that the pore-pressure is given by the following equation:

$$p(s) = -\int_{\Gamma} v_{\eta}^{*}(s,Q)p(Q)d\Gamma + \int_{\Gamma} p^{*}(s,Q)v_{\eta}(Q)d\Gamma + \int_{\Omega} p^{*}(s,q)\left[\frac{1}{M}\dot{p}(q) + b\,\mathrm{Tr}\left(\dot{\boldsymbol{\varepsilon}}(q)\right)\right]d\Omega \tag{19}$$

Considering a finite time step $\Delta t_n = t_{n+1} - t_n$ and a corresponding variable increment $\Delta X = X_{n+1} - X_n$, one can integrate equations (14), (15) and (19) along the interval Δt, leading to the following set of equations, in terms of the variable increments:

$$C_{ik}\Delta u_k(S) = \int_{\Gamma} \Delta T_k(Q)u_{ik}^{*}(S,Q)d\Gamma - \int_{\Gamma} T_{ik}^{*}(S,Q)\Delta u_k(Q)d\Gamma + \int_{\Omega} b\delta_{jk}\Delta p(q)\varepsilon_{ijk}^{*}(S,q)d\Omega + \int_{\Omega} \Delta\sigma_{jk}^{d}(q)\varepsilon_{ijk}^{*}(S,q)d\Omega \tag{20}$$

$$\Delta\sigma_{ij}(s) = -\int_{\Gamma} S_{ijk}(s,Q)\Delta u_k(Q)d\Gamma + \int_{\Gamma} D_{ijk}(s,Q)\Delta T_k(Q)d\Gamma + \int_{\Omega} R_{ijkl}(s,q)\Delta\sigma_{kl}^{d}(q)d\Omega + TL_{ij}\left[\Delta\sigma_{kl}^{d}(s)\right] + \int_{\Omega} b\delta_{kl}R_{ijkl}(s,q)\Delta p(q)d\Omega + TL_{ij}\left[b\delta_{kl}\Delta p(s)\right] \tag{21}$$

$$c(s)p(s) = -\int_{\Gamma} v_{\eta}^{*}(s,Q)p(Q)d\Gamma + \int_{\Gamma} p^{*}(s,Q)v_{\eta}(Q)d\Gamma + \frac{1}{\Delta t}\int_{\Omega}\frac{1}{M}p^{*}(s,q)\Delta p(q)d\Omega + \frac{1}{\Delta t}\int_{\Omega} b p^{*}(s,q)\mathrm{Tr}\left(\Delta\boldsymbol{\varepsilon}(q)\right)d\Omega \tag{22}$$

4 ALGEBRAIC EQUATIONS AND SOLUTION PROCEDURE

The numerical solution of the boundary value problem requires both the time and space discretizations. It should represent the system of equations in a discrete way along the linear boundary elements and into the triangular domain cells in order to obtain the approximate values of the variables of interest. One defines the number of boundary points by N_n and the number of internal nodes by N_i.

The appropriate discretization of the integrals on (20)-(22), followed by some algebraic manipulations inherent to BEM, leads to the following system:

$$[H]\{\Delta u\} = [G]\{\Delta T\} + [Q]\{\Delta\sigma^{d}\} + b[Q][IK]\{\Delta p\} \tag{23}$$

$$\{\Delta\sigma\} = -[HL]\{\Delta u\} + [GL]\{\Delta T\} + [QL]\{\Delta\sigma^{d}\} + b[QL][IK]\{\Delta p\} \tag{24}$$

$$\{p_{(i)}\} = -[HP_{(i)}]\{p\} + [GP_{(i)}]\{V\} + \frac{1}{M\Delta t}[QP_{(i)}]\{\Delta p_{(i)}\} + \frac{b}{\Delta t}[QP_{(i)}][Tr]\{\Delta\varepsilon\} \tag{25}$$

The subscript (i) refers to internal points. The influence matrices represented by $[\ ]$ come from the integration of the fundamental solutions and its derivatives. The variables represented by $\{\ \}$ are prescribed or unknown variables along the boundary or over the domain. After some arrangements, the system given above is written as

$$\left[\mathrm{E}\right]\left\{\Delta\varepsilon\right\} = \left\{\Delta\mathrm{Ns}\right\} + \left[\left[\mathrm{QS}\right] + \left[\mathrm{I}\right]\right]\left\{\Delta\sigma^{\mathrm{d}}\right\} + b\left[\left[\mathrm{QS}\right] + \left[\mathrm{I}\right]\right]\left[\mathrm{IK}\right]\left\{\Delta\mathrm{p}_{(\mathrm{i})}\right\} \tag{26}$$

$$\left[\left[\mathrm{I}\right] - \frac{1}{M\,\Delta\mathrm{t}}\left[\overline{\mathrm{QP}}_{(\mathrm{i})}\right]\right]\left\{\Delta\mathrm{p}_{(\mathrm{i})}\right\} = \left\{\overline{\mathrm{Np}}\right\} + \frac{b}{\Delta\mathrm{t}}\left[\overline{\mathrm{QP}}_{(\mathrm{i})}\right]\left[\mathrm{Tr}\right]\left\{\Delta\varepsilon\right\} \tag{27}$$

where $\left\{\Delta\mathrm{Ns}\right\}$ and $\left\{\overline{\mathrm{Np}}\right\}$ are vectors containing prescribed values and $\left[\mathrm{E}\right]$ the drained elastic tensor. Finally, arranging the two equations in a single one, in terms of $\left\{\Delta\varepsilon\right\}$ only, leads to

$$\left[\overline{\mathrm{E}}\right]\left\{\Delta\varepsilon\right\} = \left[\Delta\mathrm{Ns}\right] + \left\{\overline{\overline{\mathrm{Np}}}\right\} + \left[\overline{\mathrm{QS}}\right]\left\{\Delta\sigma^{\mathrm{d}}\right\} \tag{28}$$

which contains the new terms:

$$\left\{\overline{\overline{\mathrm{Np}}}\right\} = b\left[\overline{\mathrm{QS}}\right]\left[\mathrm{IK}\right]\left[\left[\mathrm{I}\right] - \frac{1}{M\,\Delta\mathrm{t}}\left[\overline{\mathrm{QP}}_{(\mathrm{i})}\right]\right]^{-1}\left\{\overline{\mathrm{Np}}\right\} \tag{29}$$

$$\left[\overline{\mathrm{E}}\right] = \left[\left[\mathrm{E}\right] - \frac{b^2}{\Delta\mathrm{t}}\left[\overline{\mathrm{QS}}\right]\left[\mathrm{IK}\right]\left[\left[\mathrm{I}\right] - \frac{1}{M\,\Delta\mathrm{t}}\left[\overline{\mathrm{QP}}_{(\mathrm{i})}\right]\right]^{-1}\left[\overline{\mathrm{QP}}_{(\mathrm{i})}\right]\left[\mathrm{Tr}\right]\right] \tag{30}$$

Due to the presence of correction terms associated with damage, equation (28) is non-linear at each time increment, and can be written:

$$\left\{\mathrm{Y}\left(\left\{\Delta\varepsilon_{\mathrm{n}}\right\}\right)\right\} = -\left[\overline{\mathrm{E}}\right]\left\{\Delta\varepsilon_{\mathrm{n}}\right\} + \left[\Delta\mathrm{Ns}\right] + \left\{\overline{\overline{\mathrm{Np}}}\right\} + \left[\overline{\mathrm{QS}}\right]\left\{\Delta\sigma^{\mathrm{d}}{}_{\mathrm{n}}\right\} = 0 \tag{31}$$

The solution is carried out by a Newton-Raphson's scheme. An iterative process is required to reach equilibrium. Then, from iteration i, the next try $\mathrm{i}+1$ is given by $\left\{\Delta\varepsilon_{\mathrm{n}}^{\mathrm{i}+1}\right\} = \left\{\Delta\varepsilon_{\mathrm{n}}^{\mathrm{i}}\right\} + \left\{\delta\Delta\varepsilon_{\mathrm{n}}^{\mathrm{i}}\right\}$. The correction $\left\{\delta\Delta\varepsilon_{\mathrm{n}}^{\mathrm{i}}\right\}$ is calculated from the first term of the Taylor expansion, as follows:

$$\left\{\mathrm{Y}\left(\left\{\Delta\varepsilon_{\mathrm{n}}^{\mathrm{i}}\right\}\right)\right\} + \frac{\partial\left\{\mathrm{Y}\left(\left\{\Delta\varepsilon_{\mathrm{n}}^{\mathrm{i}}\right\}\right)\right\}}{\partial\left\{\Delta\varepsilon_{\mathrm{n}}^{\mathrm{i}}\right\}}\left\{\delta\Delta\varepsilon_{\mathrm{n}}^{\mathrm{i}}\right\} = 0 \tag{32}$$

where the derivative $\dfrac{\partial\left\{\mathrm{Y}\left(\left\{\Delta\varepsilon_{\mathrm{n}}^{\mathrm{i}}\right\}\right)\right\}}{\partial\left\{\Delta\varepsilon_{\mathrm{n}}^{\mathrm{i}}\right\}}$ is the consistent tangent operator.

5 RESULTS AND DISCUSSION

5.1 Poroelastic behaviour

To illustrate the BEM formulation applied to poro-elastic media we first analyze the classic problem of one-dimensional consolidation proposed by Terzaghi, which consists of a soil column on a rigid impermeable base (Figure 1). A constant heaviside-type unit load is applied to the upper drainage surface and maintained for 100 s. Take a column of 10 m in height, consisting of Berea sandstone, completely saturated by water. The material parameters are defined in DETOURNAY & CHENG (1993). The discretization of the problem includes 44 boundary elements and 40 domain cells.

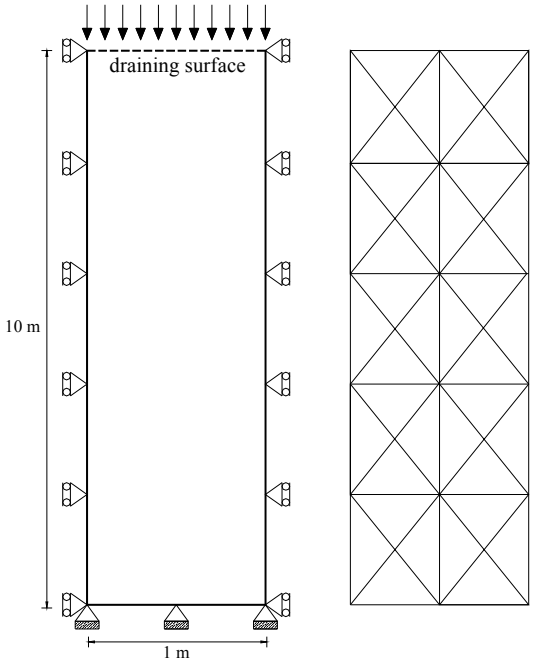

Figure 1 – Problem definition, adopted cells mesh.

From Figure 2, we can observe that the response at the initial times is characterized by the highest pore-pressure values, indicating that the fluid phase is highly requested, while the solid skeleton does not undergo all the loading action. Throughout the fluid draining process there is an increased level of effective stress, accompanied by a proportional pore-pressure decrease, until it vanishes at 100 s.

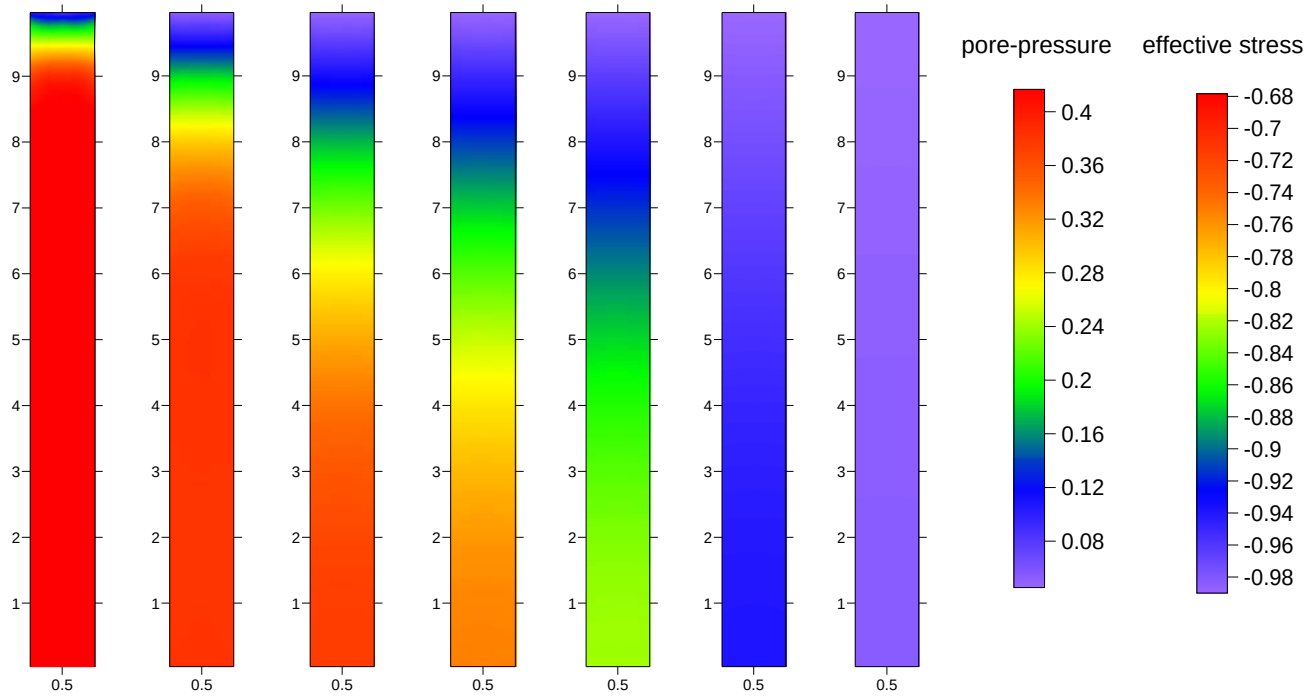

Figure 2 – Pore-pressures and vertical effective stress at 0.1 s; 1s; 5s; 10s; 20s; 50s; 100s.

Table 1 – Parameters of the Berea sandstone

Parameter	Value
G	6000 MPa
υ	0.2
υ^u	0.33
K_s	36000 MPa
ϕ_0	0.19
k	1.9×10^{-13} m^2
μ	1×10^{-9} MPa.s

Figure 3 shows the pore-pressure values at the base of the column over time. Figure 4 shows the displacement evolution at the top of the column. Both results indicate the correlation of values obtained with the formulation developed in this work, based on BEM, with the analytical response presented in DETOURNAY & CHENG (1993).

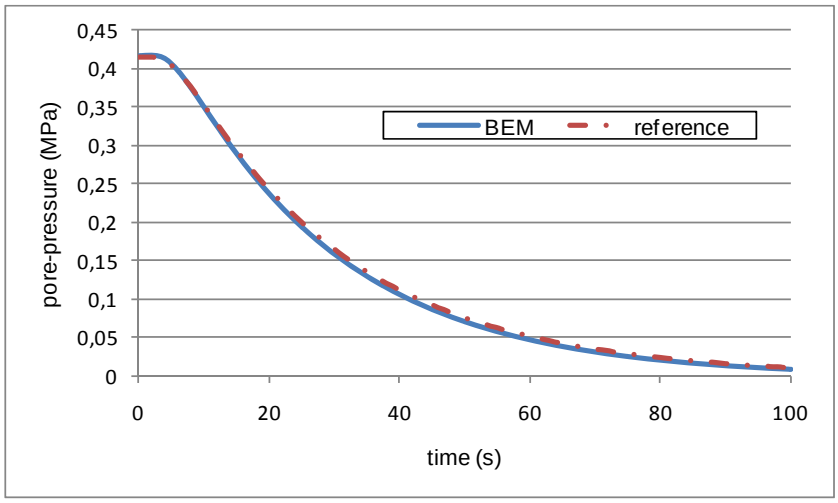

Figure 3 – Pore-pressure evolution at the base of the column.

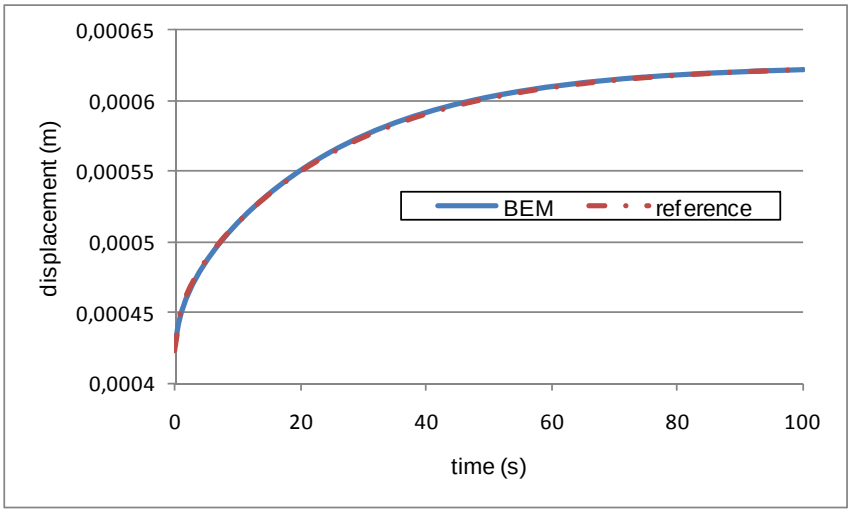

Figure 4 – Displacement evolution at the top of the column.

It should be noted that in columns of lower height the draining process, and consequently the dissipation of pore-pressures, occurs more rapidly, as shown in Figure 5, for a column 3 m in height.

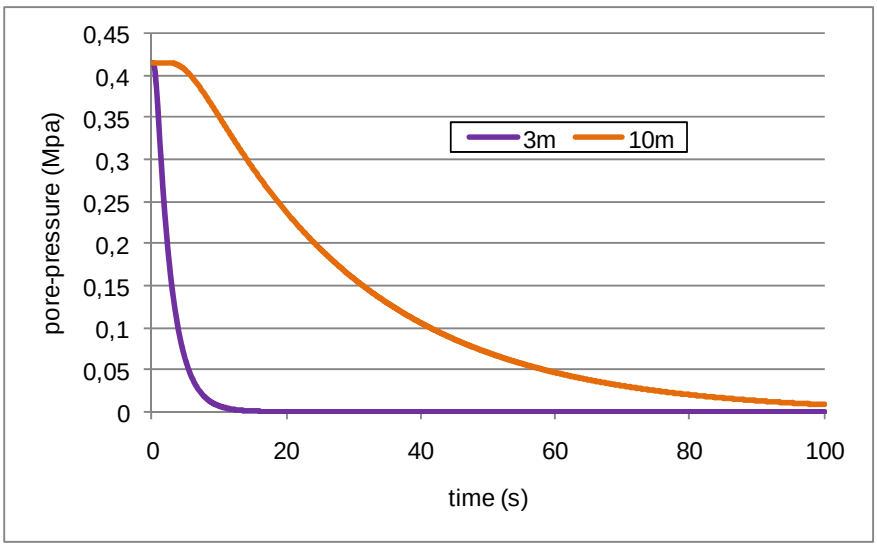

Figure 5 – Pore-pressure evolution at the base of the column, for different heights.

5.2 PORO-DAMAGE BEHAVIOUR

The overall behavior of the porodamage problem is illustrated, identifying the influences of damage in the poroelastic problem, as well as, inversely, regarding the presence of a fluid in a damaged solid problem. To this end, let us consider a column of 10 m in height, unitary width (Figure 1), consisting of Berea sandstone, whose parameters are presented in Table 1. A distributed loading equal to 15 MN/m is progressively applied over 200 s, on the upper drainage face. The damage parameters estimated for the material are of Y_0=0.001 MPa and A=0.02 MPa. The problem in question is explored by varying the drainage conditions. The incorporation of the effects resulting from the damage process to calculate the mechanical properties of the porous medium, is also considered. The mesh adopted is the one already described in 5.1.

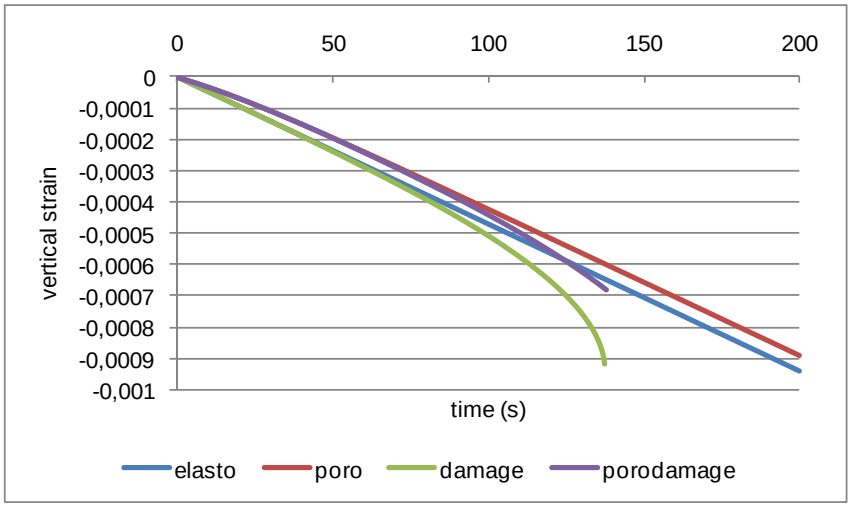

Figure 6 – Vertical strain evolution at the base of the column.

The responses regarding the four possible behaviors of the material are presented: elastic, poroelastic, elastic with damage and poroelastic coupled to damage (porodamage). It can be seen that the highest pore-pressure levels develop at the base of the column, hence strongly manifesting the problem of fluid diffusion, while, at the top of the column the damage problem is prevalent. Figure 6 shows the vertical strain curves over time at the base of the column.

In the elastic and poroelastic cases, the strains exhibit a similar behavior, except for the non-linearity induced by the flow in the poroelastic case. The difference between these two curves represents the contribution of stiffness of the fluid phase. From the comparison between the cases of damage and porodamage in Figure 6, one notes that the presence of the fluid slows the damage process, which can also be seen in Figure 7.

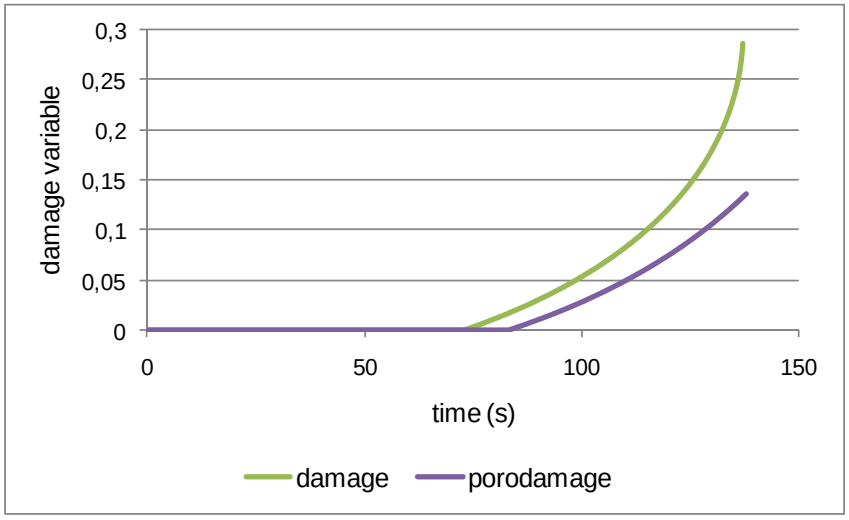

Figure 7 – Damage parameter evolution at the base of the column.

In the damage and porodamage regimes the analysis is stopped at around 140 s, when the maximum load is reached (Figure 8). In future works we intend to implement a load control strategy to capture the post-peak behavior, as for instance the arc-length scheme.

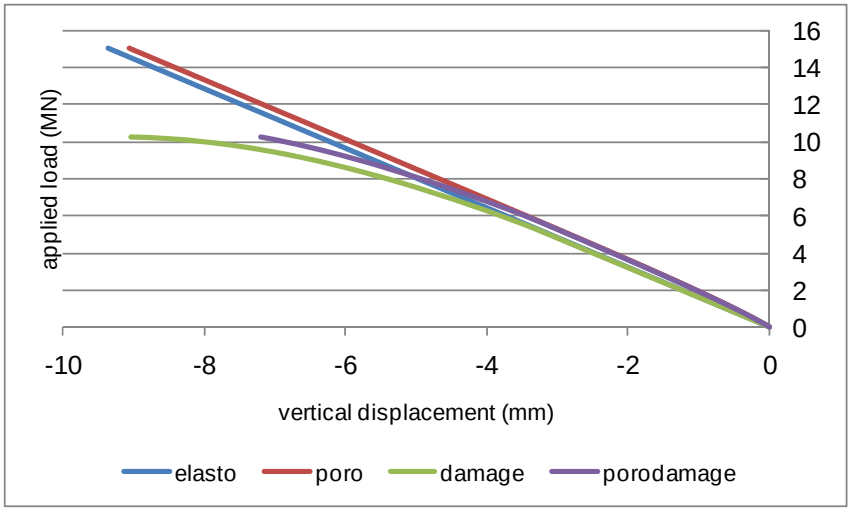

Figure 8 – Load-displacement curve at the top of the column.

It is interesting to note in Figure 9 the pore-pressure increase in the presence of damage, beyond the threshold defined in the poroelastic problem. Note in Figure 9 that the pore-pressure values are in the order of ten times smaller than the effective stress values at the base of the column.

In this case of monotonic loading, at the end of the loading process, the drainage is not yet completed, therefore there is residual pore-pressure along the column height, and the effective stress levels have not reached the value of the applied load, as shown in Figure 11. However, if the load is kept constant from 200 s on in this monotonic case, the pore-pressure will fall to zero as for the Heaviside-type load.

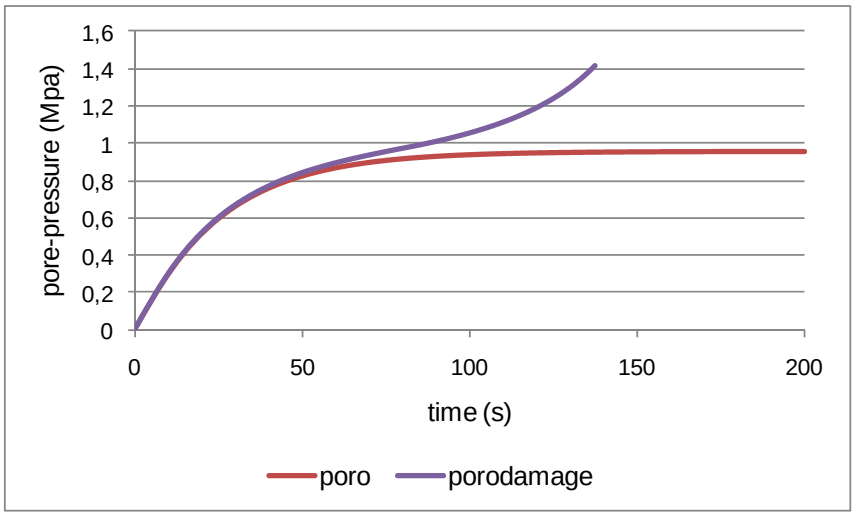

Figure 9 – Pore-pressure evolution at the base of the column.

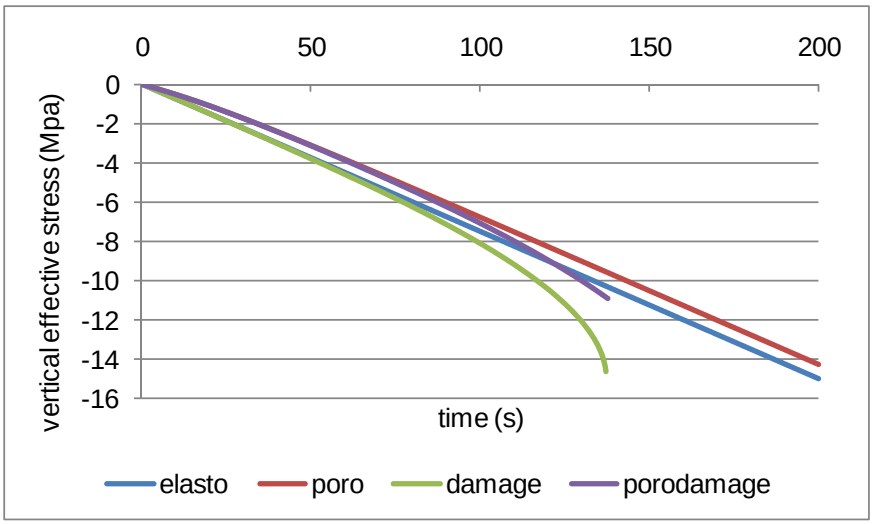

Figure 10 – Vertical effective stress evolution at the base of the column.

The overall behavior of the column essentially follows the profiles presented here for a base point, emphasizing that since the areas closer to the top of the column are examined, the damage effects prevail over the effects induced by the fluid flow .

In order to illustrate this general behavior, the distribution of the damage variable at the last instant of the analysis, at around 140 s, is shown in cases of damage and porodamage (Figure 11). In the same figure, the pore-pressure distribution in the poroelastic and porodamage case is shown, at the same instant.

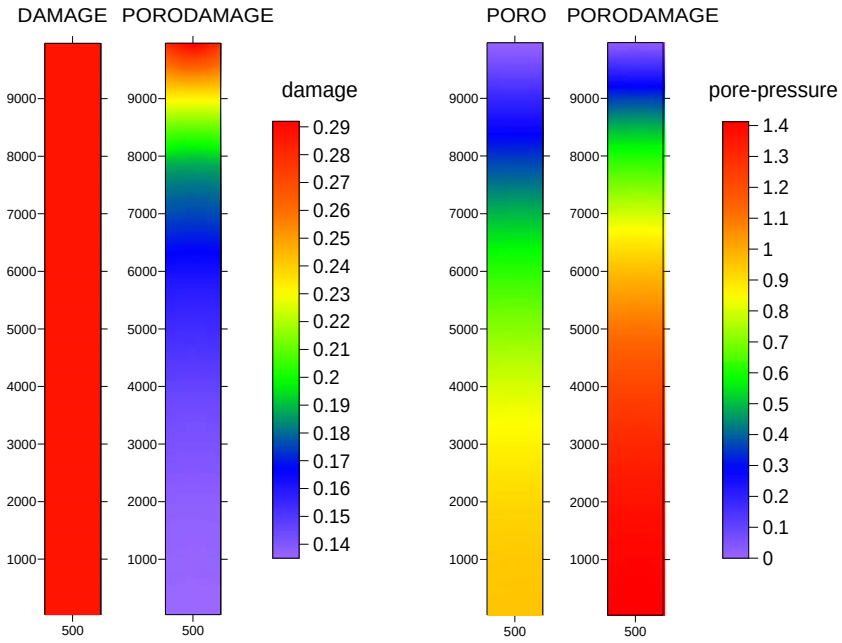

Figure 11 – Damage and pore-pressure values (MPa) at 140 s, for different regimes.

Analysis of the problem under undrained conditions. Now the analysis of the problem initially presented is proposed, impeding the fluid flow at the top of the column, that is, under undrained conditions. In this situation, regardless of the behavior adopted for the material, the response is uniform throughout the domain.

This type of boundary condition corresponds to the situation in which one can rely on the fluid stiffness throughout the whole loading process.

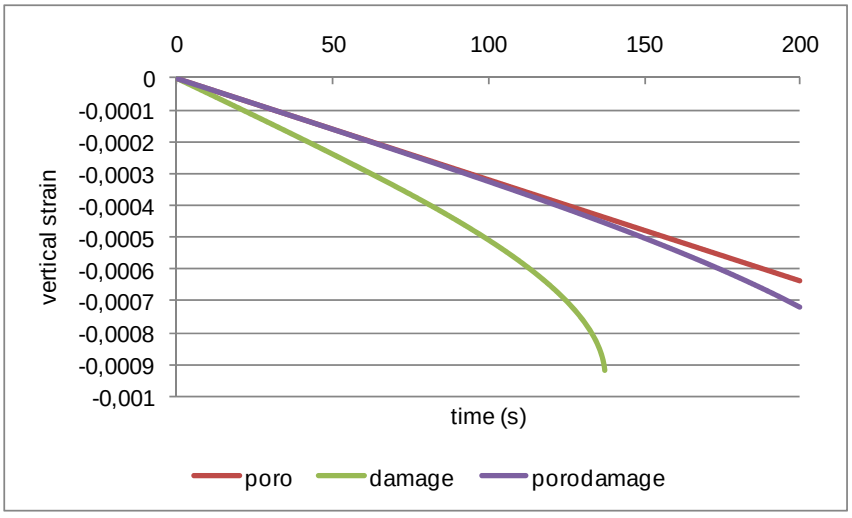

Figure 12 – Vertical strain evolution in the column.

Considering Figure 12, in which the evolution of vertical strains in the column is exhibited, it can be seen that the problem in the porodamage regime is developed up to the end of the 200 s analysis. That is, the critical load defined by the damage model was not reached. The poroelastic response in the presence of damage is significantly defined by the diffusion process, under this fluid containment condition inside the body.

The smoothing of the damage process over time is seen in Figure 13, where the evolution of the state of damage is described, considering or not the presence of the fluid. The level of damage reached at the end of 200 s, around 15%, is similar to the lowest value of damage found in the column in drained conditions (Figure 11), within a time of around 140 s.

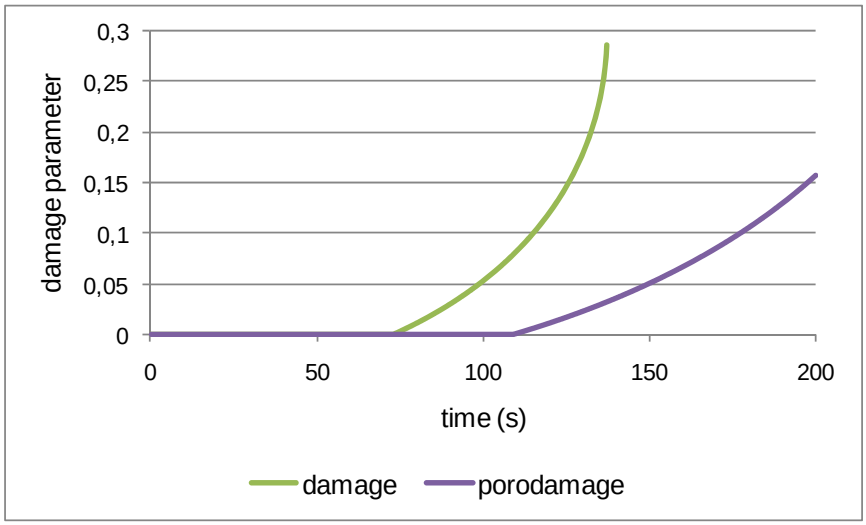

Figure 13 – Evolution of the damage variable in the column.

It is interesting to note how much higher the values of pore-pressure shown in Figure 14 are, when compared to the equivalent under drained conditions, the data is in Figure 9.

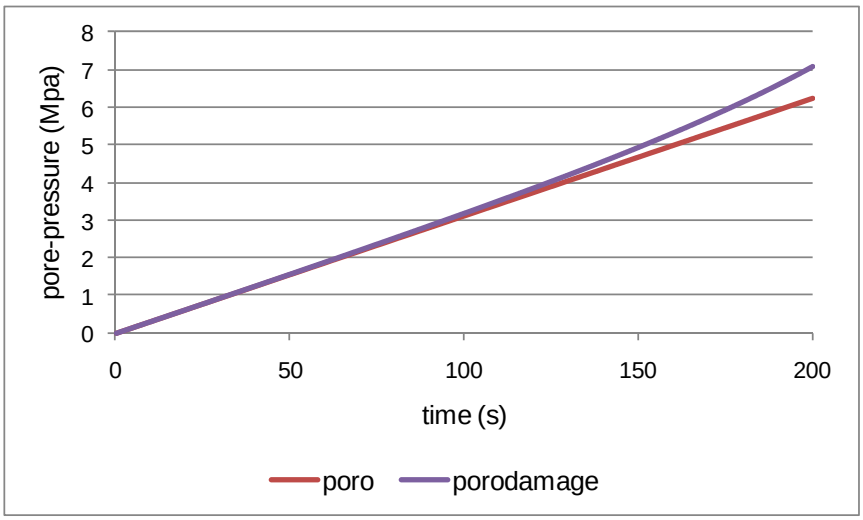

Figure 14 – Pore-pressure evolution in the column.

6 CONCLUSIONS

A BEM formulation to poro-elasto-damaged material was presented. The model has shown a reasonable level of coupling between the damage and the fluid seepage. The literature, on theoretical and experimental levels, poses several interesting questions, among which the variations that the damage state imposes on the poro-elastic parameters. Some developments in this way are being made in the presented model, in order to improve the solid-fluid interaction.

7 ACKNOWLEDGEMENTS

To CAPES, FAPESP and Île-de-France Region for the financial support.

8 REFERENCES

BENALLAL, A.; BOTTA, A. S.; VENTURINI, W. S. On the description of localization and failure phenomena by the boundary element method. **Computational Methods Applied to Mechanical Engineering**, v. 195, p. 5833-5856, 2006.

BIOT, M. A. General theory of three-dimensional consolidation. **Journal of Applied Physics**, v. 12, 1941, p. 155-164.

BOTTA, A. S.; VENTURINI, W. S.; BENALLAL, A. BEM applied to damage models emphasizing localization and associated regularization techniques. **Engineering Analysis with Boundary Elements**, v. 29, 2005, p. 814-827.

CHENG, H.; DUSSEAULT, M. B. Deformation and diffusion behaviour in a solid experiencing damage: a continous damage model and its numerical implementation. **International Journal of Rock Mechanics and Mining Science and Geomechanics**, v. 30, 1993, p. 1323-1331.

CHENG, A. H-D.; DETOURNAY, E. On singular integral equations and fundamental solutions of poroelasticity. **International Journal of Solids and Structures**, v. 35, 1998, p. 4521-4555.

CHENG, A. H-D.; LIGGETT, J. A. Boundary integral equation method for linear porous-elasticity with applications to soil consolidation. **International Journal for Numerical Methods in Engineering**, v. 20, 1984, p. 255-278.

CHENG, A. H-D.; PREDELEANU, M. Transient boundary element formulation for linear poroelasticity. **International Journal of Applied Mathematical Modelling**, v. 11, 1987, p. 285-290.

CLEARY, M. P. Fundamental solutions for a fluid-saturated porous solid. **International Journal of Solids and Structures.** v. 13, 1977, p. 785-806.

COUSSY, O. **Poromechanics. Chichester**. John Wiley and Sons, 2004.

DETOURNAY, E.; CHENG, A. H-D. Fundamentals of Poroelasticity. In: Comprehensive Rock Engineering: Principles, Practice and Projects, v. II, Analysis and Design Method, C. Fairhurst (Ed.), Pergamon Press, 1993.

GARCIA, R.; FLOREZ-LOPEZ, J.; CERROLAZ, M. A boundary element formulation for a class of non-local damage models. **International Journal of Solids and Structures**, v. 36, 1999, p. 3617-3638.

HERDING, U.; KUHN, G. A field boundary element formulation for damage mechanics. **Engineering Analysis with Boundary Elements**, v. 18**,** 1996, p. 137-147.

KACHANOV, L. M. Time of rupture process under creep conditions**. Izvestia Akademii Nauk**, n. 8, 1958, p. 26-31.

LEMAITRE, J. **A Course on Damage Mechanics**. Berlin : Springer-Verlag, 1992.

LEMAITRE, J.; CHABOCHE, J. L. **Mécanique des Matériaux Solides.** Paris: Dunod, 1985.

MARIGO, J. J. Formulation d'une loi d'endommagement d'un materiau élastique, **Comptes Rendus de l'Académie des Sciences**, v. 292 série II, 1981, p. 1309-1312.

SCHIFFMAN, R. L.; CHEN, A. T-F.; JORDAN, J. C. An analysis of consolidation theories Journal of the Soil Mechanics and Foundations Division SM 1 285-312, 1969.

SELVADURAI, A. P. S. On the mechanics of damage-susceptible poroelastic media. **Key engineering Materials**, v. 251-252, 2003, p. 363-374.

SIMO, J. C.; TAYLOR, R. L. Consistent tangent operators for rate-independent elastoplasticity. **Computer Methods in applied mechanics and Engineering**, n. 48, 1985, p. 101-118.

SLADEK, J.; SLADEK, V.; BAZANT, Z. P. Non-local boundary integral formulation for softening damage. **International Journal for Numerical Methods in Engineering**, v. 57, 2003, p. 103-116.

TERZAGHI, K. Die Berechnung der durchlassigkeitsziffer des tones aus dem verlauf der hydrodynamischen spannungserscheinungen. Sitz. Akad. Wissen., Wien Math. Naturwiss. Kl., Abt. IIa, v. 132, 1923, p. 125-138.